ACS APPLIED MATERIALS & INTERFACES

Research Article

www.acsami.org

Superior Antifouling Performance of a Zwitterionic Peptide Compared to an Amphiphilic, Non-Ionic Peptide

Huijun Ye,[†] Libing Wang,[†] Renliang Huang,[*,‡] Rongxin Su,[*,†,§,∥] Boshi Liu,[†] Wei Qi,[†,§,∥] and Zhimin He[†]

[†]State Key Laboratory of Chemical Engineering, School of Chemical Engineering and Technology, Tianjin University, Tianjin 300072, People's Republic of China

[‡]Tianjin Key Laboratory of Indoor Air Environmental Quality Control, School of Environmental Science and Engineering, Tianjin University, Tianjin 300072, People's Republic of China

[§]Collaborative Innovation Center of Chemical Science and Engineering (Tianjin), Tianjin 300072, People's Republic of China

[∥]Tianjin Key Laboratory of Membrane Science and Desalination Technology, Tianjin University, Tianjin 300072, People's Republic of China

S *Supporting Information*

ABSTRACT: The aim of this study was to explore the influence of amphiphilic and zwitterionic structures on the resistance of protein adsorption to peptide self-assembled monolayers (SAMs) and gain insight into the associated antifouling mechanism. Two kinds of cysteine-terminated heptapeptides were studied. One peptide had alternating hydrophobic and hydrophilic residues with an amphiphilic sequence of CYSYSYS. The other peptide (CRERERE) was zwitterionic. Both peptides were covalently attached onto gold substrates via gold−thiol bond formation. Surface plasmon resonance analysis results showed that both peptide SAMs had ultralow or low protein adsorption amounts of 1.97−11.78 ng/cm^2 in the presence of single proteins. The zwitterionic peptide showed relatively higher antifouling ability with single proteins and natural complex protein media. We performed molecular dynamics simulations to understand their respective antifouling behaviors. The results indicated that strong surface hydration of peptide SAMs contributes to fouling resistance by impeding interactions with proteins. Compared to the CYSYSYS peptide, more water molecules were predicted to form hydrogen-bonding interactions with the zwitterionic CRERERE peptide, which is in agreement with the antifouling test results. These findings reveal a clear relation between peptide structures and resistance to protein adsorption, facilitating the development of novel peptide-containing antifouling materials.

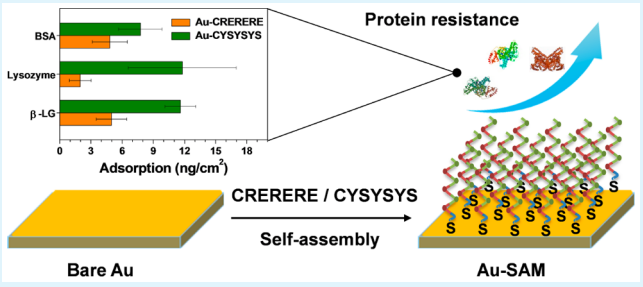

KEYWORDS: *SPR, peptides, antifouling, nonspecific adsorption, biosensor*

INTRODUCTION

The nonspecific adsorption of proteins and unwanted adhesion of cells (including bacteria) to material surfaces (often referred to as surface fouling) are ubiquitous and problematic phenomena associated with medical implantation, immunological diagnostic, biosensing, and marine coatings.[1−5] For example, during surface plasmon resonance (SPR) analysis, the surface fouling of sensor chips can mask analytic signals and greatly reduce the accuracy of quantitative results. To address this problem, a versatile strategy is to conjugate an antifouling layer to material surfaces. Over the past few decades, a number of materials have been well documented for their antifouling abilities in resisting nonspecific protein adsorption and cell adhesion, such as hydrophilic polyethylene glycol (PEG)[6,7] and zwitterionic poly(carboxybetaine methacrylate),[8,9] in which surface hydration is believed to be the dominant source of resistance to surface fouling. In general, an ideal antifouling surface should have high antifouling ability, high stability, facile preparation and modification, low cost, and in some cases, good biocompatibility and easy regeneration. However, it remains difficult for the reported antifouling surfaces to satisfy all of the above-mentioned requirements. The nonfouling mechanism of such surfaces in preventing protein/cell adhesion is also not conclusive due to complex interactions, which are generally associated with the environmental conditions, especially in complex natural media (e.g., blood). Therefore, the development of optimized approaches for designing and fabricating nonfouling surfaces has attracted considerable academic and commercial interest in recent years.

Two major classes of antifouling materials, namely hydrophilic and zwitterionic materials, have been successfully used for the development of protein/cell-resistant surfaces. Among various hydrophilic materials, oligo- and polyethylene glycol (OEG and PEG)-based molecules are commonly used.[2,10,11]

Received: July 17, 2015
Accepted: September 25, 2015
Published: September 25, 2015

DOI: 10.1021/acsami.5b06500
ACS Appl. Mater. Interfaces 2015, 7, 22448−22457

PEG-labeled surfaces offer good resistance against nonspecific protein adsorption and cell adhesion.[12] However, the difficulty of grafting PEG chains to many substrates,[13] together with easy oxidization under physiological conditions,[14,15] significantly limit their practical applications. Substantial research efforts are being devoted to the development of alternative nonfouling hydrophilic materials, such as saccharides,[16−18] polymethacrylamide,[19,20] and poly(*N*-acryloylaminoethoxyethanol).[21] For instance, we previously fabricated a protein-resistant surface by covalently grafting hyaluronic acid molecules to a gold substrate and found that ultralow or low protein adsorption of 0.6−16.1 ng/cm^2 (e.g., cow milk, 9.8 ng/cm^2) could be achieved.[18] Hydrogen bonding-induced surface hydration is considered a key attribute of the antifouling properties of such hydrophilic, nonionic molecules. Aside from hydrogen bonding, strongly ionic solvation can also generate surface hydration and thus form a tightly bound water layer, which provides a physical and energetic barrier to prevent protein adsorption and cell adhesion to the surfaces. In this respect, various zwitterionic materials carrying a positive and a negative charge on the same monomer or two different monomers have received great attention due to their high antifouling abilities, high stabilities, and facile functionalizations.[8,22−26] Among them, poly(carboxybetaine)- and poly(sulfobetaine)-based zwitterionic polymers are most widely used and have demonstrated good antifouling performance even in complex media.[4,27−30] For example, Huang et al.[29] reported a 2-layered polycarboxybetaine acrylamide (pCB) architecture, which contains a dense pCB layer and a loose pCB layer, achieving ultralow protein fouling (<5 ng/cm^2) and high antibody loading (∼1300 ng/cm^2). Some alternative zwitterionic polymers, such as poly(cysteine methacrylate),[31] have also been demonstrated to have excellent resistance to biofouling.

Peptides are composed of tandem amino acids joined with amide bonds. Thus, peptides can possess high hydrogen bond-donor/acceptor abilities due to the carbonyl, amine, and hydroxyl groups in the peptide backbone and side chains. Further, some amino acids, such as glutamic acid (E), lysine (K), and arginine (R) normally acquire a negative or positive at physiological pH, which allow for the design of zwitterionic antifouling materials using custom peptides. Therefore, some peptide-based antifouling materials, such as hydrophilic peptoids[32,33] and zwitterionic short peptides,[34−36] have been developed and exhibit high antifouling abilities due to hydrogen bonding, electrostatically induced surface hydration, or both, as discussed above. For instance, Nowinski et al.[34] designed a nonfouling zwitterionic peptide EKEKEKE-PPPPC and demonstrated that its well-defined secondary structure allows for closer packing of the monolayer with ultralow fouling properties. In this study, we investigated whether amphiphilic peptides have high antifouling abilities. We also investigated amphiphilic or zwitterionic peptides can serve as more effective surface antifouling agents.

Herein, we designed and synthesized two new heptapeptides, one of which was an amphiphilic, nonionic peptide with a sequence of CYSYSYS and the other was a zwitterionic peptide with a sequence of CRERERE. Two peptide-based SPR sensor surfaces were fabricated through grafting the heptapeptides onto gold (Au) substrates via strong gold−thiol binding. The grafting process was monitored by SPR spectroscopy, and the resulting Au-peptide surfaces were characterized using contact angle measurements and atomic force microscopy (AFM). We then evaluated the antifouling properties of both peptides by measuring nonspecific protein adsorption using single proteins (bovine serum albumin, lysozyme, and β-lactoglobulin) and natural protein-containing complexes (serum, soybean milk, and cow milk) as test samples. Moreover, to gain insight into the antifouling mechanism, we performed the molecular dynamics (MD) simulations to reveal features of the interactions between the heptapeptides and water molecules.

EXPERIMENTAL SECTION

Materials. Two heptapeptides with sequences of CYSYSYS and CRERERE were obtained from GL Biochem, Ltd. (Shanghai, China). Bovine serum albumin (BSA), lysozyme, and β-lactoglobulin were purchased from Sigma-Aldrich (Beijing, China) and used immediately upon receipt. Cow milk and soybean milk were purchased in a local market, and the protein contents were determined using a bicinchoninic acid (BCA) assay kit from the Beyotime Institute of Biotechnology (Jiangsu, China). Human blood serum was obtained from BEST-Biotech, Inc. (Tianjin, China). *N*,*N*- dimethylformamide (DMF, HPLC grade) was purchased from Guangfu Institute (Tianjin, China). The water used in all experiments was prepared in a three-stage Millipore Milli-Q Plus 185 purification system (Millipore Corp., Bedford, MA) and had a resistivity greater than 18 MΩ cm. The pH values of all solutions were measured with a MP220 pH meter (Mettler Toledo, Switzerland). All solutions were filtered using syringe filters with 0.22 μm diameter pores before use. All other chemicals were obtained from commercial sources.

Fabrication of Au-CYSYSYS and Au-CRERERE Surfaces. BK7 glass substrates were deposited with a 2 nm chromium layer followed by a 50 nm -gold layer, using an electron-beam evaporator (Temescal, CA) and a base pressure of 10^{-6} Torr. The deposition rates for the chromium and gold layers were 0.5 and 1 Å/s, respectively. The resulting bare gold substrates were cleaned by immersion in freshly prepared Piranha solution (7:3 v/v mixture of concentrated sulfuric acid and 30% hydrogen peroxide) for 2 h, rinsed with anhydrous ethanol and ultrapure water, and dried under high-purity nitrogen. The pretreated gold substrates were then stored in an enclosed container at 4 °C until use. As a cautionary note, Piranha solution is extremely corrosive and reacts violently with organic materials. Thus, it should be handled with great care.

Phosphate buffered saline (PBS, pH 7.4; 10 mM phosphate, 138 mM sodium chloride, and 2.7 mM potassium chloride) and DMF were prepared and degassed with nitrogen for 1 h before use. The CYSYSYS and CRERERE peptides were dissolved in the DMF and PBS solutions, respectively, to a final concentration of 4 mg/mL. Then, the pretreated and cleaned bare gold substrates were immersed in the peptide solutions and incubated for 12 h at 25 °C. The resulting surfaces, denoted as Au-CYSYSYS and Au-CRERERE, respectively, were then rinsed thoroughly with anhydrous ethanol, dried with nitrogen, and stored in an enclosed container at 4 °C until use.

Measurements of Nonspecific Protein Adsorption by SPR. To evaluate the performance of the Au-peptide surfaces in resisting protein adsorption, we used six different test samples, including three single-protein solutions and three naturally occurring complex media. BSA, lysozyme, and β-lactoglobulin were individually dissolved in PBS to final concentrations of 1 mg/mL. Soybean milk, cow milk, and blood serum were centrifuged three times (20 min/centrifugation step) at 5000 rpm in a 3−18K centrifuge (Sigma, Germany) to remove particulate matter and then diluted to 1 mg/mL with PBS solution. The concentrations of proteins in these media before and after dilution were measured using a BCA protein assay.

A time-resolved (TR) SPR spectrometer (DyneChem HiTech Ltd., Changchun, China) equipped with a 650 nm laser as the light source was used to measure the real-time adsorption of proteins onto the Au-peptide surfaces. A baseline signal was established by flowing PBS over the Au-peptide surfaces at a flow rate of 50 μL/min for approximately 30 min. The protein-containing solution was injected into the flow cell at a flow rate of 10 μL/min for 10 min, followed by a cleaning with PBS solution at 50 μL/min for 10 min. During this process, the SPR angle shifts were recorded as $\Delta\theta$ values, which were used to quantify

DOI: 10.1021/acsami.5b06500
ACS Appl. Mater. Interfaces 2015, 7, 22448−22457

Scheme 1. (a) Molecular structures of an Amphiphilic Peptide with a Sequence of CYSYSYS and a Zwitterionic Peptide with a Sequence of CRERERE and (b) Schematic Illustration of the Attachment of Peptide Self-Assembled Monolayers (SAMs) on the Au Surfaces

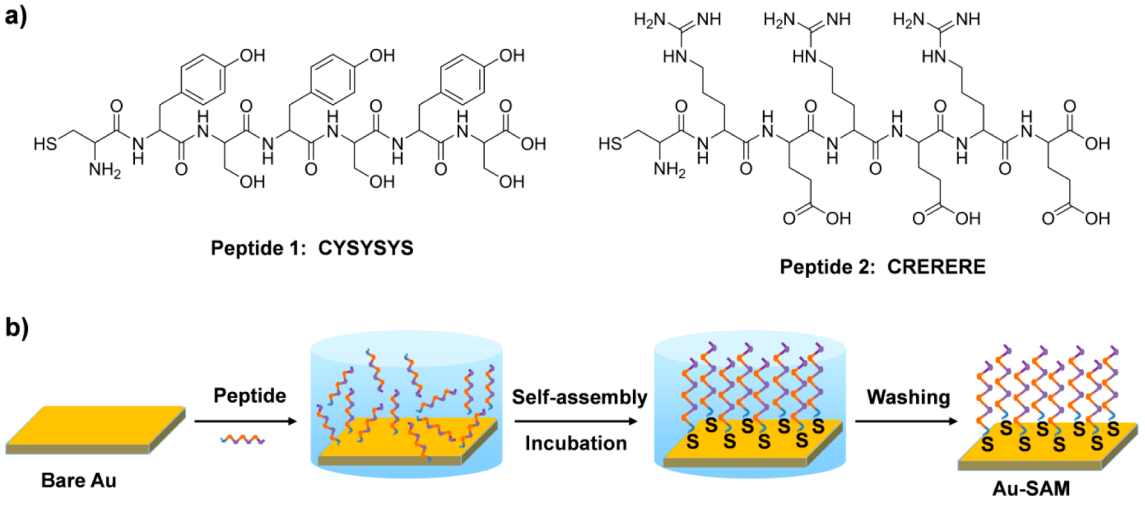

the amount of protein adsorption. For this TR-SPR system, a shift in SPR angle of 0.12° corresponded to a surface coverage of 100 ng/cm^2, which was estimated by comparing the infrared reflection/absorption spectra with a known amount of BSA deposited on the gold surface.[12,18] The detection limit for the TR-SPR system is 0.0015°, which represents a surface coverage of 1.25 ng/cm^2. In addition, the surface area of the SPR sensor is 28.26 mm^2 and the volume of the flow cell is 55.95 mm^3.

Characterization. To monitor the modification of peptides onto gold surfaces, the SPR angles of different surfaces, including bare Au, Au-CYSYSYS, and Au-CRERERE, were measured by SPR spectroscopy in angle-scanning mode. PBS was used as running buffer to perform these experiments.

The Au-peptide surfaces were characterized by X-ray photoelectron spectroscopy (XPS) using an ESCALAB 250Xi spectrometer (Thermo Fisher Scientific, Waltham, MA). The X-ray gun operated at 15 kV and 150 W power, and the diameter of the analysis area was approximately 500 μm. The exposure time was kept constant at 104 s to avoid damaging the samples. Survey spectra were recorded in the range of 800−100 eV, using 1.0 eV steps and 100 ms dwell times. High-resolution C 1s, N 1s, O 1s, and S 2p spectra were collected with a step size of 0.1 eV. The results were analyzed using CasaXPS software.

The static contact angles were measured using an OCA15EC device (DataPhysics Instruments, Germany), equipped with SCA 202 software. All contact angles were measured with a 1 μL water droplet deposited on test surfaces at ambient temperature. The contact angle was calculated by curve fitting the profile of the droplet from the three-phase interface of the image captured by a CCD camera. The values presented represent averages of four separate measurements recorded at different areas on each substrate.

The surface topography of bare Au, Au-CYSYSYS, and Au-CRERERE was characterized by AFM in contact mode using an Agilent 5500 atomic force microscope (Agilent, Santa Clara, CA) equipped with N9797 AU-1FP Pico software. Silicon nitride AFM tips (NP-S; Bruker AFM Probes, Billerica, MA) with an elastic modulus of 0.58 N/m were used to conduct the experiments.

Attenuated total reflection-Fourier transform infrared spectroscopy (ATR-FTIR) spectra were acquired using Spectra-Tech's HATR single-angle reflection accessory in conjunction with a MAGNA-560 spectrometer (Nicolet). Each spectrum was collected with a minimum of 200 scans at a resolution of 4 cm^{-1}. Each sample was analyzed three times. The ATR-FTIR spectrum of bare gold was recorded and subtracted from the original spectra of Au-peptide samples.

Circular dichroism (CD) analysis was performed on a Jasco J-810 CD spectropolarimeter (Jasco Inc., Japan) over a wavelength range of 190−270 nm at 25 °C with a resolution of 0.1 nm. Spectra were recorded three times using a scanning speed of 50 nm/min. To prepare the sample, the CRERERE peptide was dissolved in PBS solution with a final concentration of 0.25 mg/mL.

Zeta potential measurements of CRERERE solutions at different pH values were performed using a Zetasizer NanoZS instrument equipped with a streaming potential cell (Malvern Instruments, UK). PBS solutions with pH values ranging from 3 to 10 were prepared by adding potassium hydrogen phthalate/hydrochloric acid (pH = 3−4), disodium hydrogen phosphate/potassium dihydrogen phosphate (pH = 5−8), or sodium carbonate/sodium bicarbonate (pH = 9−10). A pH meter (MP220, Mettler-Toledo, Switzerland) was used to measure the pH values of the solutions. The Zeta potentials were measured at 28 °C, and the value presented for each pH value represents an average of at least three independent measurements.

MD Simulations. For MD simulations, hydrogen atoms were added to peptide residues using tLeaP. The system was centered in a cubic TIP3P water box of 60 × 60 × 60 Å. A sufficient number of Na^+ ions were added to neutralize the negative charges in the system. FF99SB force field was used to assign peptides. MD simulation was performed using the NAMD2.9 software package. The system was first minimized by 5000 steps of steepest-decent minimization, followed by an additional 5000 steps with a conjugate gradient. After energy minimization, the system was heated to the target temperature of 300 K for a period of 20 ps under constant-pressure periodic boundary conditions and equilibrated using 5 ns of constant pressure and temperature (NPT) with time step of 1 fs, which was followed by 100 ns of production simulation performed under the same conditions. A cutoff of 10 Å was used for nonbonded interactions, and long-range electrostatic interactions were treated by means of the Particle Mesh Ewald method. The MD simulation results were analyzed using the ptraj program in the AmberTools 14 package and visual molecular dynamics (VMD).

RESULTS AND DISCUSSION

In this work, we designed an amphiphilic peptide and a zwitterionic heptapeptide with N-terminal cysteine residues (Scheme 1a). The amphiphilic heptapeptide (CYSYSYS) contained alternating hydrophobic tyrosine (Y) and hydrophilic serine (S) residues, while the zwitterionic heptapeptide (CRERERE) contained alternating positive arginine residues (R) and negative glutamic acid residues (E). Scheme 1b illustrates the strategy used to attach the amphiphilic and zwitterionic peptides onto the Au substrates. Specifically, the bare Au substrate was incubated in either peptide solution for

DOI: 10.1021/acsami.5b06500
ACS Appl. Mater. Interfaces 2015, 7, 22448−22457

12 h. During this process, the peptide molecules were directly attached to the Au surface via covalent Au−S bonds formed between Au surface and the thiol groups of each peptide, leading to the formation of a peptide self-assembled monolayer (SAM). To confirm the surface attachment, we employed SPR spectroscopy to measure changes in the SPR angles, which are highly sensitive to refractive index differences within 200 nm above the Au surface. As shown in Figure 1, the SPR angle of

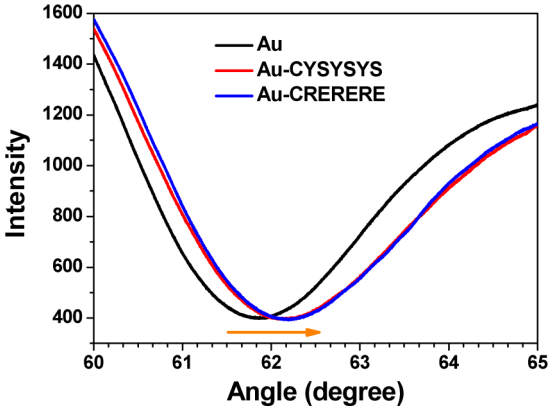

Figure 1. SPR angle scanning spectra of bare a Au surface (black line), a CYSYSYS-modified Au surface (red line), and a CRERERE-modified surface (blue line).

the bare Au surface was 61.86°, which was shifted to 62.15 and 62.18° after formation of the CYSYSYS and CRERERE peptide SAMs, respectively, corresponding to deposition densities of ~241 ng/cm^2 (1.66 × 10^{14} molecules/cm^2) and ~266 ng/cm^2 (1.64 × 10^{14} molecules/cm^2), which are close to the maximum values (Figure S1). The observed increases in the SPR angles provided direct evidence of the successful attachment of peptide SAMs onto the Au surfaces.

To further evaluate the attachment of peptide SAMs, we used XPS to monitor changes in surface chemistries. As shown in Figure 2 and Figure S2, the binding energies of the S 2p3/2 and S 2p1/2 peaks were 161.1 and 162.7 eV, respectively, for both Au-peptide SAM surfaces, which corresponded to bound sulfur atoms existing as thiolate species rather than physically adsorbed thiols on the Au surfaces.[37,38] As expected, no S 2p peak was observed on the bare Au surfaces. Additionally, XPS data showed that the photoelectron signals of the Au substrates (Au 4f) decreased after peptide modification, indicative of surface coverage with a peptide SAM (Figure S2). The lower Au signal for the Au-CYSYSYS surface, together with higher signaling for the O, N, and S elements, indicated that such peptide SAM surfaces were more densely packed compared to the CRERERE-derived peptide SAM surface. In addition to Au-thiol bond formation, hydrophobic interactions between the CYSYSYS peptide and the Au surface may have contributed to the facile attachment of peptide chains onto the Au surface.

To characterize the wettabilities of the peptide SAM surfaces, the static water contact angles of bare Au, Au-CYSYSYS, and Au-CRERERE surfaces were measured. As summarized in Table 1, the bare Au surface was hydrophobic and had a water

Table 1. Static Water Contact Angles of Bare Au, Au-CYSYSYS, and Au-CRERERE Surfaces

Surfaces	Photographs	Contact angles (°)
Au		100.9 ± 3.6
Au-CYSYSYS		39.7 ± 1.1
Au-CRERERE		19.6 ± 0.4

contact angle of 100.9°. Attachment of the CYSYSYS peptide SAM led to a much lower contact angle of 39.7°, presumably due to the influence of the hydrophilic chemical groups (e.g., OH, NH) in the peptide chains. In contrast, the zwitterionic CRERERE peptide SAM had a lower contact angle of 19.6° and displayed marked hydrophilicity, which was likely attributable to the unique zwitterionic structure carrying alternate amino (NH_2) and carboxyl (COOH) groups. The contact angles of such peptide SAMs were near the reported values of other antifouling peptides, such as an EKEKEKEPPPPC peptide SAM (20°)[36] and a 3-MPA-HHHDD−OH peptide SAM (35°).[39]

The uniformity of the attached peptide SAMs on the gold substrates was assessed by AFM imaging. As shown in Figure 3, the AFM images showed that both peptide SAMs had a smooth surface with a characteristic root-mean-squared roughness of 0.8 nm, which was similar to that of the bare Au surface (0.7 nm), indicating uniform coverage of the Au surface. No peptide aggregates were observed in the AFM images, which may explain the enhanced antifouling properties of peptide SAMs. As shown in Figure S3, the peak−peak roughness of CRERERE peptide SAM and CYSYSYS peptide SAM is calculated as 5.1 and 6.4 nm, respectively. Additionally, the molecular simulation (Discovery Studio) results show that the fully extended lengths

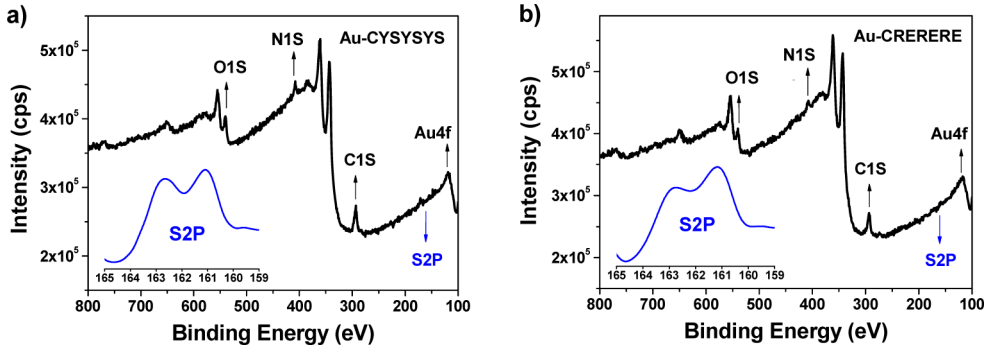

Figure 2. XPS survey spectra of (a) Au-CYSYSYS and (b) Au-CRERERE surfaces. (Insets) Corresponding XPS high-resolution spectra for S 2p.

DOI: 10.1021/acsami.5b06500
ACS Appl. Mater. Interfaces 2015, 7, 22448−22457

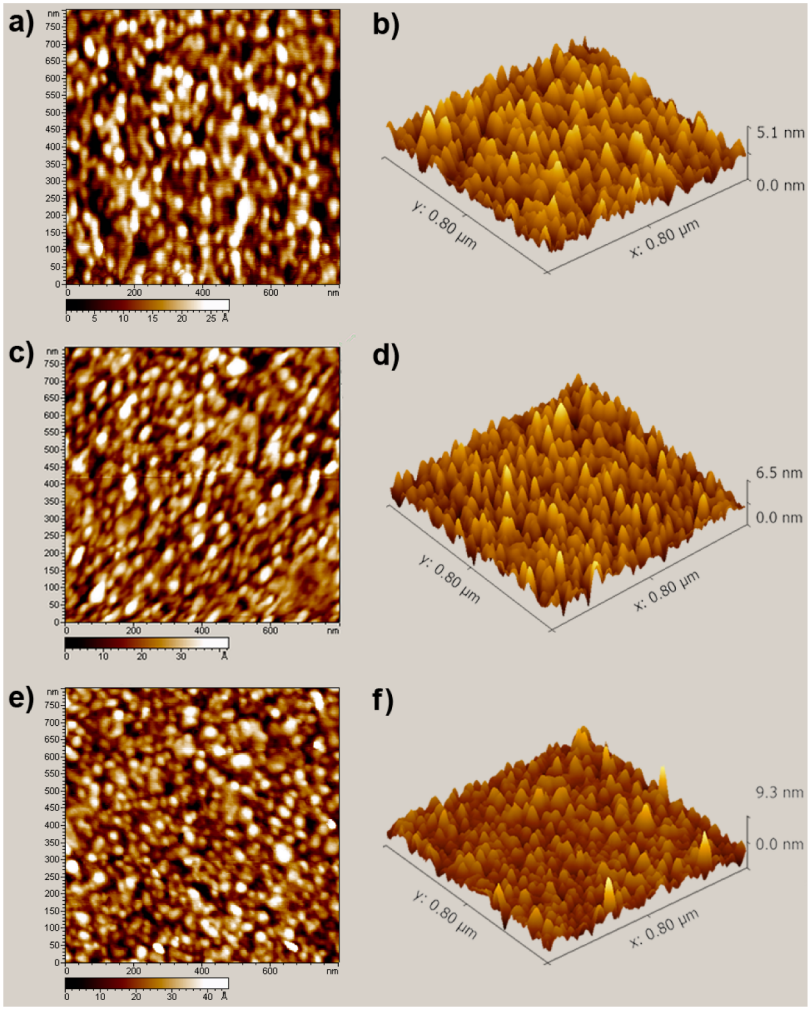

Figure 3. Flattened and topographic AFM images of (a and b) bare Au, (c and d) Au-CRERERE, and (e and f) Au-CYSYSYS.

of CRERERE and CYSYSYS peptide were 3.57 and 3.18 nm, respectively. Therefore, the sum of peak−peak roughness and fully extended peptide length gives 8.67 nm for the zwitterionic CRERERE peptide SAM, which is similar to the value of amphiphilic CYSYSYS peptide SAM (9.58 nm). In this case, we expect that the surface roughness of the peptide SAM has no significant effect on their antifouling performance.

To assess the antifouling abilities of the peptide SAMs, SPR spectroscopy was employed to measure nonspecific protein adsorption of three different proteins, including BSA (M_w = 66 kDa, pI = 4.7), lysozyme (M_w = 14.7 kDa, pI = 11), and β-lactoglobulin (M_w = 18.4 kDa, pI = 5.2). Briefly, the SPR surface (bare Au, Au-peptide SAMs) was exposed to PBS, which served as a running buffer to establish a baseline. Then, 100 μL of each protein solution (1 mg/mL) was injected and flowed over the surface at a flow rate of 10 μL/min, followed by a cleaning with PBS at a flow rate of 50 μL/min. Figure 4 and Figure S4 show real-time SPR signals (indicated as the angle shift, $\Delta\theta$) resulting from protein adsorption and desorption. For both peptide SAMs, the single proteins caused an angle shift ranging from 0.004 to 0.017°, which was much smaller than observed with the bare Au surface (~0.2° for BSA, Figure 4a,b and Figure S4a). In our SPR system, a 0.12° angle shift corresponds to 100 ng/cm^2 of surface coverage. Therefore, the adsorption of BSA on the bare Au surface could be calculated as 167 ng/cm^2, while the corresponding values of BSA adsorption on peptide SAMs were significantly decreased to a range of 3−14 ng/cm^2. In comparison with amphiphilic CYSYSYS peptide SAM, the zwitterionic CRERERE peptide SAM showed a higher antifouling capacity, which was evidenced by smaller angle shifts observed during the entire adsorption−desorption process.

Figure 5a summarizes the nonspecific adsorption of the single BSA, lysozyme, and β-lactoglobulin proteins on the peptide SAMs. In the control experiments, the bare Au surface had high adsorption in these protein solutions (Table S1). As shown in Figure 5a, both the CYSYSYS and CRERERE peptide SAMs effectively resisted BSA adsorption down to a level of 7.75 and 4.8 ng/cm^2, respectively, which is comparable to or lower than that of previously studied antifouling surfaces, such as hyaluronic acid (7.7 ng/cm^2) and dextran (15.4 ng/cm^2).[18] The nonspecific adsorption of lysozyme and β-lactoglobulin on the CYSYSYS peptide SAM was 11.78 and 11.6 ng/cm^2, respectively, while the corresponding protein-adsorption values on CRERERE peptide SAMs decreased to 1.95 and 4.97 ng/cm^2, respectively. Although the protein species studied had differing molecular weights and isoelectric points, the zwitterionic peptide SAM exhibited better antifouling performance against BSA, lysozyme, and β-lactoglobulin. In addition, it is noteworthy that all nonspecific protein adsorption on the zwitterionic CRERERE peptide SAM was below the commonly accepted ultralow fouling criterion of <5 ng/cm^2 and similar to

DOI: 10.1021/acsami.5b06500
ACS Appl. Mater. Interfaces 2015, 7, 22448−22457

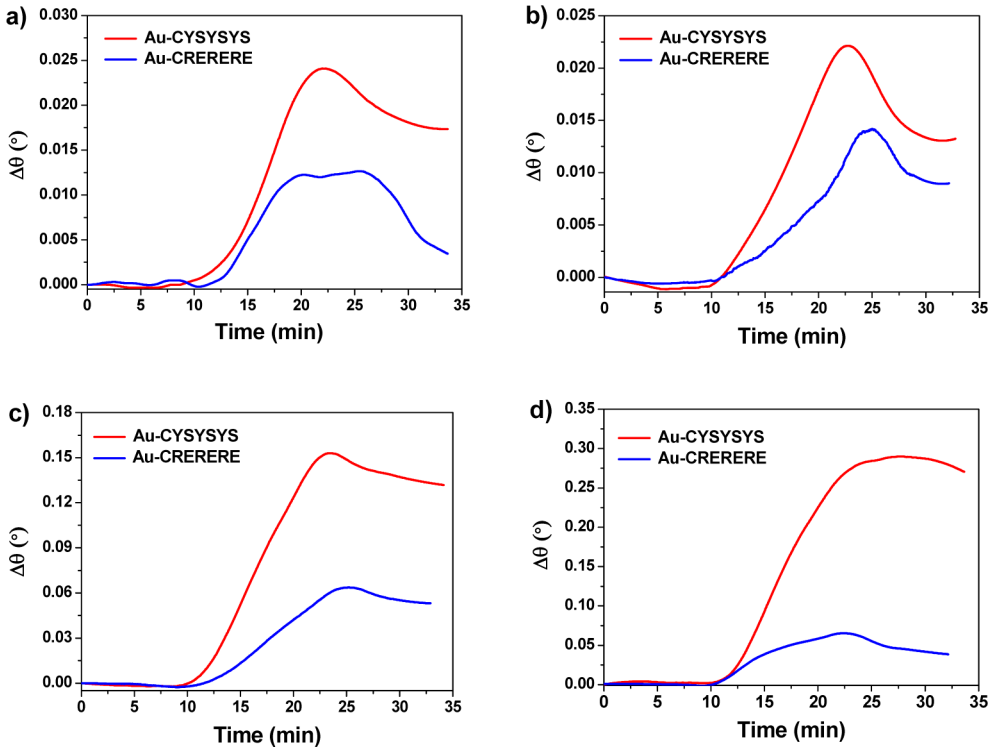

Figure 4. SPR sensorgrams showing nonspecific protein adsorption of single protein solutions, including (a) lysozyme (1 mg/mL) and (b) β-lactoglobulin (1 mg/mL). SPR sensorgrams were also generated in the presence of natural complex media, including (c) serum (1 mg/mL) and (d) cow milk (1 mg/mL). SPR sensorgrams were acquired using Au-CYSYSYS and Au-CRERERE surfaces.

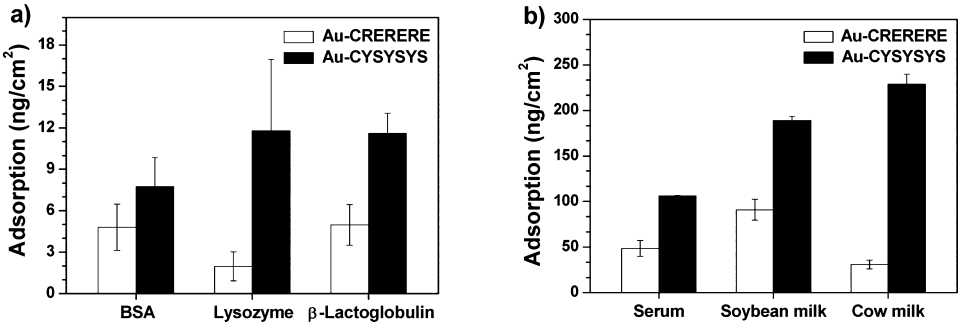

Figure 5. Nonspecific protein adsorption observed with (a) single-protein solutions (BSA, lysozyme, and β-lactoglobulin) and (b) natural complex media (serum, soybean milk, and cow milk). Each error bar represents the standard deviation of three independent measurements.

that of the typical hydrophilic/zwitterionic surfaces (Table S2), such as zwitterionic EKEKEKEPPPPC peptide (e.g., lysozyme, 3.5 ng/cm^2)[34] and zwitterionic polymers.[4]

We further evaluated the antifouling properties of peptide SAMs in natural protein complex-containing media, including human blood serum, cow milk, and soybean milk. Table S3 summarizes the protein concentrations of these samples. To provide a direct comparison with the single-protein systems, these natural media were diluted to a final protein concentration of 1 mg/mL in PBS. Figure 4c,d and Figure S4b show real-time SPR signals observed when testing diluted blood serum, cow milk, and soybean milk. It was observed that the protein complexes caused large SPR responses on the CYSYSYS and CRERERE peptide SAMs. The nonspecific protein adsorption levels of these media to bare Au surfaces and peptide SAMs are summarized in Table S1 and Figure 5b. Although both peptide SAMs exhibited large protein adsorptions with serum (e.g., 48.4 and 106.1 ng/cm^2) presumably due to the presence of large proteins and other macromolecules (e.g., polysaccharides), the data also indicated that the CRERERE peptide had greater antifouling ability than the CYSYSYS peptide, consistent with the results observed with single proteins. Overall, the designed amphiphilic and zwitterionic peptide SAMs demonstrated excellent antifouling performances against protein adsorption using single-protein solutions. These findings provide direct evidence to support our hypothesis that amphiphilic peptides also have good antifouling abilities. Furthermore, the results indicated that the zwitterionic peptide caused reduced fouling compared to amphiphilic peptide, regardless of whether single proteins or natural protein complexes were used.

To understand the influence of the peptide structure on the antifouling behaviors of peptide SAMs, we examined the secondary structure of peptides on Au surfaces using ATR-FTIR. The ATR-FTIR spectra of the CYSYSYS and CRERERE peptides showed maximum peaks for amide I bands at 1669 ±

DOI: 10.1021/acsami.5b06500
ACS Appl. Mater. Interfaces 2015, 7, 22448−22457

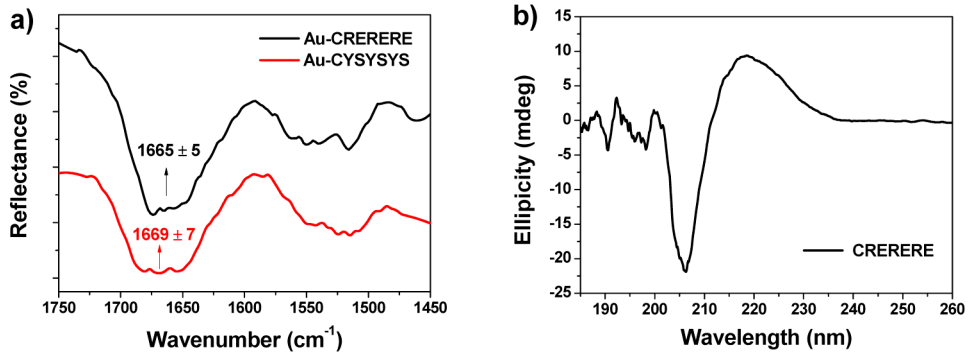

Figure 6. (a) Representative ATR-FTIR spectra for the (black) CRERERE and (red) CYSYSYS peptide SAMs attached to Au surfaces. (b) CD spectrum of the CRERERE peptide dissolved in PBS at a concentration of 0.25 mg/mL.

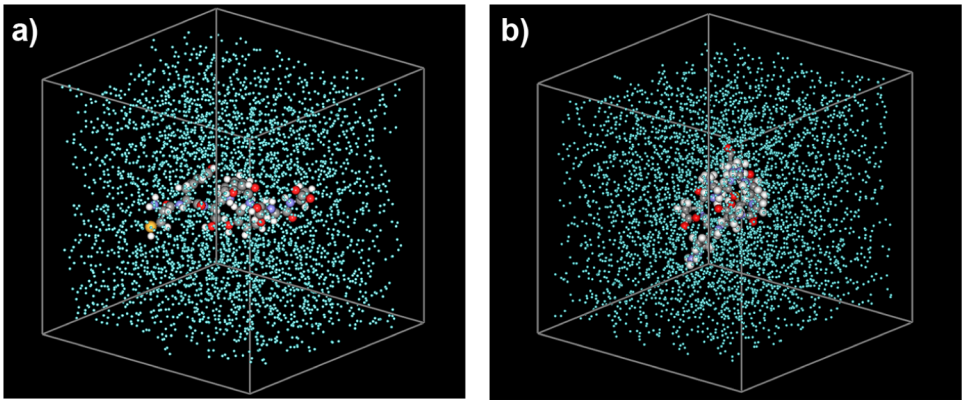

Figure 7. Snapshots from MD simulations of a solution of (a) CYSYSYS and (b) CRERERE in water at T = 300 K, showing a change in water density within the cubic TIP3P water box.

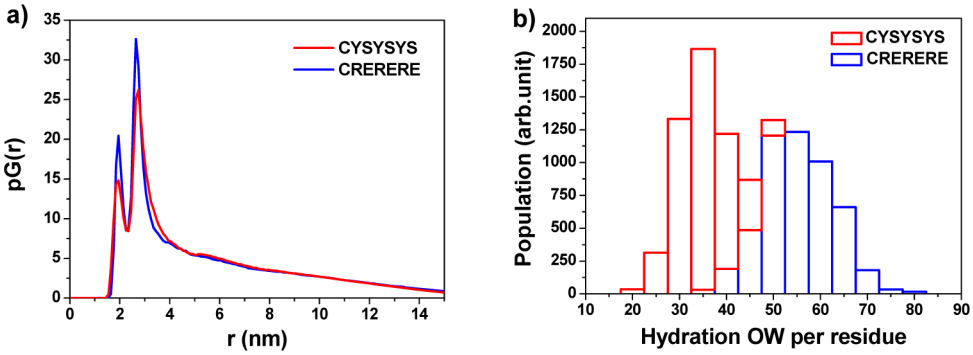

Figure 8. (a) The proximal radial distribution, pG(r), of water oxygen atoms surrounding the (red) CYSYSYS and (blue) CRERERE peptides. (b) Distribution of the average number of water oxygen atoms within the first hydration layer of the CYSYSYS and CRERERE peptides, as determined by MD simulations.

7 and 1665 ± 5 cm^{-1} (Figure 6a), respectively, which are higher than that of α-helical structures with a typical amide I band at 1650−1658 cm^{-1}. In addition, the CD spectrum of the CRERERE peptide also indicated that no regular α-helical or β-sheet structure was formed (Figure 6b). These results suggest that both peptides likely adopt a disordered, random configuration on the Au surface.[40,41] A similar result was also observed previously with an EKEKEKE-C peptide.[34] In addition to the secondary structure, the zeta potentials of the CRERERE peptide were also measured at different pH values to confirm its zwitterionic property. As shown in Figure S5, the CRERERE peptide has an isoelectric point (pI) of approximately 6.5 and acquires a positive or negative zeta potential when the pH values deviate from the pI.

The zwitterionic charged structure is essential for electrostatically induced surface hydration, which contributes to the prevention of protein adsorption. However, for the short amphiphilic CYSYSYS peptide, unlike a previously described amphiphilic polymer,[42,43] the real-time SPR signal (Figure 4) did not show significantly enhanced fouling release from the SAM surface during the PBS-washing step compared to the zwitterionic peptide, presumably due to the lack of the fluorinated moieties that could lead to a lower surface free energy so as to the fouling release. Therefore, we expect that the good antifouling performance of the amphiphilic peptide was mainly attributable to hydrogen bonding-induced surface hydration.

DOI: 10.1021/acsami.5b06500
ACS Appl. Mater. Interfaces 2015, 7, 22448−22457

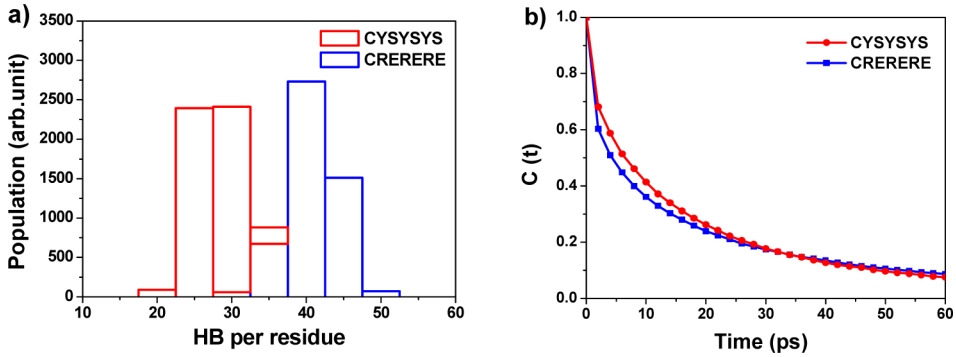

Figure 9. (a) Distribution of the average number of hydrogen bonds formed between CYSYSYS or CRERERE and water, as determined by MD simulations. (b) Autocorrelation functions of hydrogen bonds for (red) CYSYSYS and (blue) CRERERE, calculated from MD simulations.

To test whether a hydration layer forms around the peptide chain and thus plays a significant role in preventing protein adsorption, we performed extensive atomistic MD simulations with the amphiphilic and zwitterionic peptides in explicit water for 100 ns. The snapshots from the MD simulations showed that the water density gradually increased as the water molecules tightly surrounded the peptide molecules (Figure 7). The average conformations of both peptides are shown in Figure S6. Figure 8a shows the proximal radial distribution functions (pG[r])[33,44,45] of oxygen atoms in water molecules surrounding the hydrogen-bonding atoms of the CYSYSYS and CRERERE peptides.Both peptides displayed first hydration peaks at the positions of 2.05 and 2.85 Å. The nearly identical peak positions for both peptides suggested that the water molecules formed similar hydration shells. However, the intensity of the hydration peak with CRERERE was much higher than that observed with CYSYSYS, indicative of a higher local water density within the first two hydration shells around the CRERERE peptide. The average distributions of the water molecules in the first hydration layer around each peptide are summarized in Figure 8b. The average number of water molecules around the zwitterionic CRERERE peptide was 55, while that for the amphiphilic CYSYSYS peptide was 35.

The stability of the water layers formed around the peptides are reflected by the average number and lifetime of the hydrogen bonds formed between each peptide and the attendant water molecules.[33] Figure 9a shows the distributions of the number of CYSYSYS-water and CRERERE- water hydrogen bonds. The average number of hydrogen bonds for the CYSYSYS-water and CRERERE-water pairs was 30 and 40, respectively. All hydrogen bonds formed are summarized in Tables S4 and S5, which clearly show donor/acceptor atoms of each hydrogen bond and reveal that more hydrogen bonds are predicted to form between the CRERERE peptide and water molecules, as compared to that for the CYSYSYS peptide–water system. The lifetimes of the hydrogen bonds were calculated using the autocorrelation function $C(t)$ of the hydrogen-bond operator $h(t)$.[33,45] As shown in Figure 9b, the autocorrelations of the hydrogen bonds in the CYSYSYS–water and CRERERE–water systems were found to decay slowly. The relaxation time of the hydrogen bonds, defined as the time corresponding to the autocorrelation of e^{-1}, was 12.749 ps for CYSYSYS–water and 10.418 ps for CRERERE–water, both of which were much larger than that for water–water hydrogen bonds.[33] The relatively long-lived hydration layer around each peptide is a good indicator of antifouling activity because it is difficult for proteins to displace hydrogen-bonded water molecules. The somewhat larger relaxation times observed for the amphiphilic peptide-water hydrogen bonds indicated a stronger binding affinity of water to the CYSYSYS peptide, compared to the CRERERE peptide. Overall, the MD simulation results provide powerful evidence to support the importance of hydration layers in resisting protein adsorption, regardless of whether amphiphilic and zwitterionic peptides are used. Compared with the amphiphilic CYSYSYS peptide, the zwitterionic CRERERE peptide forms a larger number of hydrogen bonds with water, which is in accordance with its higher antifouling performance described above. In addition, the strong binding affinity of water to the CYSYSYS peptide suggests this structure as a potential antifouling motif.

CONCLUSIONS

In summary, we fabricated two types of novel protein-resistant surfaces by grafting amphiphilic CYSYSYS and zwitterionic CRERERE peptides to Au substrates and demonstrated that both peptide SAM surfaces showed good antifouling performances against the nonspecific adsorption of single-protein solutions. An ultralow (<5 ng/cm^2) or low (<12 ng/cm^2) protein adsorption on these surfaces was observed with BSA, lysozyme, β-lactoglobulin solutions. A comparative SPR analysis indicated that the zwitterionic peptide SAM had a higher resistance to protein adsorption than did the amphiphilic peptide SAM, regardless of whether single or natural complex protein media were tested. Moreover, the MD simulation results demonstrated the existence of strongly bound water molecules around the peptide chains, which likely play an important role in fouling resistance through the inhibition of protein–surface interactions. In comparison with the amphiphilic peptide, the zwitterionic peptide formed a higher number of hydrogen bonds with water molecules, which is in accordance with its better antifouling performance. The results presented in this study shed insights into the underlying antifouling mechanism and should inform the design of more effective peptide-containing antifouling materials in the future.

ASSOCIATED CONTENT

Supporting Information

The Supporting Information is available free of charge on the ACS Publications website at DOI: 10.1021/acsami.5b06500.

Adsorption amounts of peptides on bare Au surfaces with different peptide concentrations, XPS surface compositions, AFM images of the peptide SAMs, SPR sensorgrams showing the nonspecific protein adsorption onto Au-peptide surfaces, Zeta potentials of the CRERERE

DOI: 10.1021/acsami.5b06500
ACS Appl. Mater. Interfaces 2015, 7, 22448–22457

peptide, the molecular conformations of CRERERE and CYSYSYS peptide in water, the nonspecific adsorption from single protein solutions and protein complexes-containing media on bare Au surface, summary of the antifouling surfaces and the corresponding nonspecific protein adsorption, the concentrations of proteins in milk, soybean milk, and human serum blood, summary of hydrogen bonds in the CYSYSYS peptide and CRERERE peptide. (PDF)

AUTHOR INFORMATION

Corresponding Authors

*E-mail: tjuhrl@tju.edu.cn.

*E-mail: surx@tju.edu.cn. Tel: +86 22 27407799. Fax: +86 22 27407599.

Notes

The authors declare no competing financial interest.

ACKNOWLEDGMENTS

This work was supported by the Ministry of Science and Technology of China (Nos. 2012YQ090194, 2012AA06A303, and 2012BAD29B05), the Natural Science Foundation of China (Nos. 51473115, 21276192, and 21306134) and the Ministry of Education (Nos. NCET-11-0372 and 20130032120029).

REFERENCES

(1) Blaszykowski, C.; Sheikh, S.; Thompson, M. Surface Chemistry to Minimize Fouling from Blood-Based Fluids. *Chem. Soc. Rev.* **2012**, *41*, 5599−5612.

(2) Banerjee, I.; Pangule, R. C.; Kane, R. S. Antifouling Coatings: Recent Developments in the Design of Surfaces That Prevent Fouling by Proteins, Bacteria, and Marine Organisms. *Adv. Mater.* **2011**, *23*, 690−718.

(3) Krishnamoorthy, M.; Hakobyan, S.; Ramstedt, M.; Gautrot, J. E. Surface-Initiated Polymer Brushes in the Biomedical Field: Applications in Membrane Science, Biosensing, Cell Culture, Regenerative Medicine and Antibacterial Coatings. *Chem. Rev.* **2014**, *114*, 10976−11026.

(4) Jiang, S.; Cao, Z. Ultralow-Fouling, Functionalizable, and Hydrolyzable Zwitterionic Materials and Their Derivatives for Biological Applications. *Adv. Mater.* **2010**, *22*, 920−932.

(5) Zhang, Z.; Zhang, M.; Chen, S.; Horbett, T. A.; Ratner, B. D.; Jiang, S. Blood Compatibility of Surfaces with Superlow Protein Adsorption. *Biomaterials* **2008**, *29*, 4285−4291.

(6) Sileika, T. S.; Kim, H. D.; Maniak, P.; Messersmith, P. B. Antibacterial Performance of Polydopamine-Modified Polymer Surfaces Containing Passive and Active Components. *ACS Appl. Mater. Interfaces* **2011**, *3*, 4602−4610.

(7) Emilsson, G.; Schoch, R. L.; Feuz, L.; Hook, F.; Lim, R. Y.; Dahlin, A. B. Strongly Stretched Protein Resistant Poly(Ethylene Glycol) Brushes Prepared by Grafting-To. *ACS Appl. Mater. Interfaces* **2015**, *7*, 7505−7515.

(8) Ladd, J.; Zhang, Z.; Chen, S.; Hower, J. C.; Jiang, S. Zwitterionic Polymers Exhibiting High Resistance to Nonspecific Protein Adsorption from Human Serum and Plasma. *Biomacromolecules* **2008**, *9*, 1357−1361.

(9) Zhao, C.; Zhao, J.; Li, X.; Wu, J.; Chen, S.; Chen, Q.; Wang, Q.; Gong, X.; Li, L.; Zheng, J. Probing Structure−Antifouling Activity Relationships of Polyacrylamides and Polyacrylates. *Biomaterials* **2013**, *34*, 4714−4724.

(10) Li, L.; Yan, B.; Yang, J.; Chen, L.; Zeng, H. Novel Mussel-Inspired Injectable Self-Healing Hydrogel with Anti-Biofouling Property. *Adv. Mater.* **2015**, *27*, 1294−1299.

(11) Kim, S.; Gim, T.; Kang, S. M. Versatile, Tannic Acid-Mediated Surface Pegylation for Marine Antifouling Applications. *ACS Appl. Mater. Interfaces* **2015**, *7*, 6412−6416.

(12) Pop-Georgievski, O.; Verreault, D.; Diesner, M.-O.; Proks, V.; Heissler, S.; Rypacek, F.; Koelsch, P. Nonfouling Poly(Ethylene Oxide) Layers End-Tethered to Polydopamine. *Langmuir* **2012**, *28*, 14273−14283.

(13) Greene, G. W.; Martin, L. L.; Tabor, R. F.; Michalczyk, A.; Ackland, L. M.; Horn, R. Lubricin: A Versatile, Biological Anti-Adhesive with Properties Comparable to Polyethylene Glycol. *Biomaterials* **2015**, *53*, 127−136.

(14) Webster, R.; Didier, E.; Harris, P.; Siegel, N.; Stadler, J.; Tilbury, L.; Smith, D. PEGylated Proteins: Evaluation of Their Safety in the Absence of Definitive Metabolism Studies. *Drug. Metab. Dispos.* **2007**, *35*, 9−16.

(15) Arima, Y.; Toda, M.; Iwata, H. Complement Activation on Surfaces Modified with Ethylene Glycol Units. *Biomaterials* **2008**, *29*, 551−560.

(16) Ederth, T.; Ekblad, T.; Pettitt, M. E.; Conlan, S. L.; Du, C.-X.; Callow, M. E.; Callow, J. A.; Mutton, R.; Clare, A. S.; D'Souza, F.; et al. Resistance of Galactoside-Terminated Alkanethiol Self-Assembled Monolayers to Marine Fouling Organisms. *ACS Appl. Mater. Interfaces* **2011**, *3*, 3890−3901.

(17) Fyrner, T.; Lee, H. H.; Mangone, A.; Ekblad, T.; Pettitt, M. E.; Callow, M. E.; Callow, J. A.; Conlan, S. L.; Mutton, R.; Clare, A. S.; Konradsson, P.; Liedberg, B.; Ederth, T. Saccharide-Functionalized Alkanethiols for Fouling-Resistant Self-Assembled Monolayers: Synthesis, Monolayer Properties, and Antifouling Behavior. *Langmuir* **2011**, *27*, 15034−15047.

(18) Liu, X.; Huang, R.; Su, R.; Qi, W.; Wang, L.; He, Z. Grafting Hyaluronic Acid onto Gold Surface to Achieve Low Protein Fouling in Surface Plasmon Resonance Biosensors. *ACS Appl. Mater. Interfaces* **2014**, *6*, 13034−13042.

(19) Liu, Q.; Singh, A.; Lalani, R.; Liu, L. Ultralow Fouling Polyacrylamide on Gold Surfaces Via Surface-Initiated Atom Transfer Radical Polymerization. *Biomacromolecules* **2012**, *13*, 1086−1092.

(20) Cringus-Fundeanu, I.; Luijten, J.; van der Mei, H. C.; Busscher, H. J.; Schouten, A. J. Synthesis and Characterization of Surface-Grafted Polyacrylamide Brushes and Their Inhibition of Microbial Adhesion. *Langmuir* **2007**, *23*, 5120−5126.

(21) Chen, H.; Zhang, M.; Yang, J.; Zhao, C.; Hu, R.; Chen, Q.; Chang, Y.; Zheng, J. Synthesis and Characterization of Antifouling Poly(N-Acryloylaminoethoxyethanol) with Ultralow Protein Adsorption and Cell Attachment. *Langmuir* **2014**, *30*, 10398−10409.

(22) Zhang, Z.; Chen, S.; Jiang, S. Dual-Functional Biomimetic Materials: Nonfouling Poly (Carboxybetaine) with Active Functional Groups for Protein Immobilization. *Biomacromolecules* **2006**, *7*, 3311−3315.

(23) Chen, S.; Zheng, J.; Li, L.; Jiang, S. Strong Resistance of Phosphorylcholine Self-Assembled Monolayers to Protein Adsorption: Insights into Nonfouling Properties of Zwitterionic Materials. *J. Am. Chem. Soc.* **2005**, *127*, 14473−14478.

(24) Chen, S.; Yu, F.; Yu, Q.; He, Y.; Jiang, S. Strong Resistance of a Thin Crystalline Layer of Balanced Charged Groups to Protein Adsorption. *Langmuir* **2006**, *22*, 8186−8191.

(25) Gao, C.; Li, G.; Xue, H.; Yang, W.; Zhang, F.; Jiang, S. Functionalizable and Ultra-Low Fouling Zwitterionic Surfaces Via Adhesive Mussel Mimetic Linkages. *Biomaterials* **2010**, *31*, 1486−1492.

(26) Cheng, G.; Xue, H.; Zhang, Z.; Chen, S.; Jiang, S. A Switchable Biocompatible Polymer Surface with Self-Sterilizing and Nonfouling Capabilities. *Angew. Chem., Int. Ed.* **2008**, *47*, 8831−8834.

(27) Mi, L.; Jiang, S. Integrated Antimicrobial and Nonfouling Zwitterionic Polymers. *Angew. Chem., Int. Ed.* **2014**, *53*, 1746−1754.

(28) Cao, Z.; Jiang, S. Super-Hydrophilic Zwitterionic Poly-(Carboxybetaine) and Amphiphilic Non-Ionic Poly(Ethylene Glycol) for Stealth Nanoparticles. *Nano Today* **2012**, *7*, 404−413.

DOI: 10.1021/acsami.5b06500
ACS Appl. Mater. Interfaces 2015, 7, 22448−22457

(29) Huang, C. J.; Li, Y.; Jiang, S. Zwitterionic Polymer-Based Platform with Two-Layer Architecture for Ultra Low Fouling and High Protein Loading. *Anal. Chem.* **2012**, *84*, 3440−3445.
(30) Shao, Q.; Jiang, S. Molecular Understanding and Design of Zwitterionic Materials. *Adv. Mater.* **2015**, *27*, 15−26.
(31) Alswieleh, A. M.; Cheng, N.; Canton, I.; Ustbas, B.; Xue, X.; Ladmiral, V.; Xia, S.; Ducker, R. E.; El Zubir, O.; Cartron, M. L.; Hunter, C. N.; Leggett, G. J.; Armes, S. P. Zwitterionic Poly(Amino Acid Methacrylate) Brushes. *J. Am. Chem. Soc.* **2014**, *136*, 9404−9413.
(32) Lin, S.; Zhang, B.; Skoumal, M. J.; Ramunno, B.; Li, X.; Wesdemiotis, C.; Liu, L.; Jia, L. Antifouling Poly(Beta-Peptoid)S. *Biomacromolecules* **2011**, *12*, 2573−2582.
(33) Ham, H. O.; Park, S. H.; Kurutz, J. W.; Szleifer, I. G.; Messersmith, P. B. Antifouling Glycocalyx-Mimetic Peptoids. *J. Am. Chem. Soc.* **2013**, *135*, 13015−13022.
(34) Nowinski, A. K.; Sun, F.; White, A. D.; Keefe, A. J.; Jiang, S. Sequence, Structure, and Function of Peptide Self-Assembled Monolayers. *J. Am. Chem. Soc.* **2012**, *134*, 6000−6005.
(35) Chen, S.; Cao, Z.; Jiang, S. Ultra-Low Fouling Peptide Surfaces Derived from Natural Amino Acids. *Biomaterials* **2009**, *30*, 5892−5896.
(36) Cui, J.; Ju, Y.; Liang, K.; Ejima, H.; Lorcher, S.; Gause, K. T.; Richardson, J. J.; Caruso, F. Nanoscale Engineering of Low-Fouling Surfaces through Polydopamine Immobilisation of Zwitterionic Peptides. *Soft Matter* **2014**, *10*, 2656−2663.
(37) Ishida, T.; Hara, M.; Kojima, I.; Tsuneda, S.; Nishida, N.; Sasabe, H.; Knoll, W. High Resolution X-Ray Photoelectron Spectroscopy Measurements of Octadecanethiol Self-Assembled Monolayers on Au(111). *Langmuir* **1998**, *14*, 2092−2096.
(38) Ishida, T.; Choi, N.; Mizutani, W.; Tokumoto, H.; Kojima, I.; Azehara, H.; Hokari, H.; Akiba, U.; Fujihira, M. High-Resolution X-Ray Photoelectron Spectra of Organosulfur Monolayers on Au(111): S(2p) Spectral Dependence on Molecular Species. *Langmuir* **1999**, *15*, 6799−6806.
(39) Bolduc, O. R.; Pelletier, J. N.; Masson, J.-F. o. Spr Biosensing in Crude Serum Using Ultralow Fouling Binary Patterned Peptide Sam. *Anal. Chem.* **2010**, *82*, 3699−3706.
(40) Duevel, R. V.; Corn, R. M. Amide and Ester Surface Attachment Reactions for Alkanethiol Monolayers at Gold Surfaces as Studied by Polarization Modulation Fourier Transform Infrared Spectroscopy. *Anal. Chem.* **1992**, *64*, 337−342.
(41) Sakurai, T.; Oka, S.; Kubo, A.; Nishiyama, K.; Taniguchi, I. Formation of Oriented Polypeptides on Au (111) Surface Depends on the Secondary Structure Controlled by Peptide Length. *J. Pept. Sci.* **2006**, *12*, 396−402.
(42) Weinman, C. J.; Gunari, N.; Krishnan, S.; Dong, R.; Paik, M. Y.; Sohn, K. E.; Walker, G. C.; Kramer, E. J.; Fischer, D. A.; Ober, C. K. Protein Adsorption Resistance of Anti-Biofouling Block Copolymers Containing Amphiphilic Side Chains. *Soft Matter* **2010**, *6*, 3237−3243.
(43) Wong, S. Y.; Han, L.; Timachova, K.; Veselinovic, J.; Hyder, M. N.; Ortiz, C.; Klibanov, A. M.; Hammond, P. T. Drastically Lowered Protein Adsorption on Microbicidal Hydrophobic/Hydrophilic Polyelectrolyte Multilayers. *Biomacromolecules* **2012**, *13*, 719−726.
(44) Wei, T.; Carignano, M. A.; Szleifer, I. Lysozyme Adsorption on Polyethylene Surfaces: Why Are Long Simulations Needed? *Langmuir* **2011**, *27*, 12074−12081.
(45) Ebbinghaus, S.; Kim, S. J.; Heyden, M.; Yu, X.; Heugen, U.; Gruebele, M.; Leitner, D. M.; Havenith, M. An Extended Dynamical Hydration Shell around Proteins. *Proc. Natl. Acad. Sci. U. S. A.* **2007**, *104*, 20749−20752.

DOI: 10.1021/acsami.5b06500
ACS Appl. Mater. Interfaces 2015, 7, 22448−22457